J Physiol 589.15 (2011) pp 3837–3854

The Journal of Physiology

Multiple extra-synaptic spillover mechanisms regulate prolonged activity in cerebellar Golgi cell–granule cell loops

Tahl Holtzman[1,2], Vanessa Sivam[1], Tian Zhao[1], Oivier Frey[4], Peter Dow van der Wal[4], Nico F. de Rooij[4], Jeffrey W. Dalley[2,3] and Steve A. Edgley[1]

[1] *Department of Physiology, Development and Neuroscience, Downing Street, University of Cambridge CB2 3DY, UK*
[2] *Behavioural and Clinical Neuroscience Institute and Department of Experimental Psychology, University of Cambridge, Downing Street, Cambridge CB2 3EB, UK*
[3] *Department of Psychiatry, University of Cambridge, Addenbrooke's Hospital, Cambridge CB2 2QQ, UK*
[4] *Sensors, Actuators and Microsystems Laboratory, Institute of Microengineering (IMT), Ecole Polytechnique Federale de Lausanne, CH-2000 Neuchâtel, Switzerland*

Non-technical summary The cerebellar cortex contains complex neural circuits related to information processing for the learning and control of movements. We show that the interaction between the main input neurones, the granule cells and their inhibitory counterparts, the Golgi cells, is far more complex than previously thought. Traditionally, granule cells are considered to excite Golgi cells, thereby forming a negative feedback loop. In contrast, our study reveals that granule cell input to Golgi cells is predominantly *inhibitory*, through the action of specialised glutamate receptors expressed in Golgi cells. These results force a re-evaluation of our current best theories of how the cerebellar circuitry processes information.

Abstract Despite a wealth of *in vitro* and modelling studies it remains unclear how neuronal populations in the cerebellum interact *in vivo*. We address the issue of how the cerebellar input layer processes sensory information, with particular focus on the granule cells (input relays) and their counterpart inhibitory interneurones, Golgi cells. Based on the textbook view, granule cells *excite* Golgi cells via glutamate forming a negative feedback loop. However, Golgi cells express inhibitory mGluR2 receptors suggesting an inhibitory role for glutamate. We set out to test this glutamatergic paradox in Golgi cells. Here we show that granule cells and Golgi cells interact through extra-synaptic signalling mechanisms during sensory information processing, as well as synaptic mechanisms. We demonstrate that such interactions depend on granule cell-derived glutamate acting via inhibitory mGluR2 receptors leading causally to the suppression of Golgi cell activity for several hundreds of milliseconds. We further show that granule cell-derived inhibition of Golgi cell activity is regulated by GABA-dependent extra-synaptic Golgi cell inhibition of granule cells, identifying a regulatory loop in which glutamate and GABA may be critical regulators of Golgi cell–granule cell functional activity. Thus, granule cells may promote their own prolonged activity via paradoxical *feed-forward* inhibition of Golgi cells, thereby enabling information processing over long timescales.

(Received 10 February 2011; accepted after revision 9 June 2011; first published online 13 June 2011)
Corresponding author T. Holtzman: Dept of Experimental Psychology, Downing Street, Cambridge CB2 3EB, UK. Email: th247@cam.ac.uk

Abbreviations APICA, (*RS*)-1-amino-5-phospho-noindan-1-carboxylic acid; CUSUM, cumulative sum; LLD, long-lasting depression; LLE, long-lasting excitation; GSE, glutamate-sensing electrode; mGluR, metabotropic glutamate receptor; NSE, non-sensing electrode; PSTH, post-stimulus time histogram; SLD, short-lasting depression; SLE, short-lasting excitation; THIP, 4,5,6,7-tetrahydroisoxazolo[5,4-c]pyridin-3-ol.

DOI: 10.1113/jphysiol.2011.207167

Introduction

As arguably the best described brain microcircuit, the cerebellum offers a unique platform from which questions about how neural circuits process information can be investigated. Although basic connectivity is well described, detailed *in vitro* analysis of the interactions between cerebellar cortical neurones have revealed unusual properties, including extra-synaptic spillover and metabotropic modulation (Rossi & Hamann, 1998; Tempia *et al*. 1998; Mitchell & Silver, 2000*a*, *b*; Watanabe & Nakanishi, 2003). How these phenomena contribute to cerebellar cortical information processing is poorly understood.

One of the roles for the cerebellar cortex is to generate appropriately timed signals, which is implicit for a role generating coordinated motor outputs. This is exemplified by classically conditioned eye-blink learning, a cerebellar-dependent form of associative learning that requires generation of behaviour that is precisely delayed by 100–1000 ms (optimally 200–300 ms), following a salient conditional stimulus (see Yeo & Hesslow, 1998; Ohyama *et al*. 2003; Thompson & Steinmetz, 2009). Based on its serial connections, cerebellar cortex is usually modelled as a fast input–output device, so how cellular activity can be generated on such long timescales is subject to speculation (see Medina & Mauk, 2000; Yamazaki & Tanaka, 2009).

Our previous work described long-lasting depressions in Golgi cell activity with accompanying long-lasting increases in Purkinje cell output following single-pulse somatosensory stimulation (Holtzman *et al*. 2006). We hypothesise that long-lasting *disinhibition* of granule cells arising during Golgi cell depressions drives the long-lasting Purkinje cell responses and thereby opens up processing over long timescales. Here we describe the mechanisms underlying the long duration of these responses and reveal a complex interplay between granule and Golgi cells involving extra-synaptic spillover and metabotropic modulation.

Golgi cells are of pivotal importance in normal cerebellar function as they directly influence the mossy fibre excitatory input (granule cells) to the cortex. Since Golgi cells inhibit granule cells, they have been considered as negative *feedback* controllers, regulating granule cell responsiveness to match the ambient mossy fibre activity (Eccles *et al*. 1966; Marr, 1969; Albus, 1971). This might filter mossy fibre input patterns (Gabbiani *et al*. 1994; Mitchell & Silver, 2000*b*) and potentially determine granule cell oscillatory firing (Maex & De Schutter, 1998). Long-lasting depression responses in Golgi cells evoked by the same stimuli may diminish levels of spillover-mediated tonic inhibition in granule cells (Brickley *et al*. 1996; Crowley *et al*. 2009), thus allowing a gain-increase in their input–output relationship over a longer time-course (Mitchell & Silver, 2003).

In this study we show that spillover glutamate, derived at least in part from granule cells, directly underpins long-lasting depressions of Golgi cell firing, via mGluR2-mediated inhibition (see Watanabe & Nakanishi, 2003), in parallel with glycinergic inhibition mediated by Lugaro cells (see Dumoulin *et al*. 2001). These findings challenge the widely accepted view that Golgi cells regulate granule cells via *feedback* control, suggesting instead a regulatory loop where granule cells may facilitate their own prolonged activity by paradoxical *feed-forward* inhibition of Golgi cells.

Methods

All procedures were approved by the local ethical review panel of the University of Cambridge and by UK Home Office regulations. Experiments were performed, *in vivo*, on 54 adult Wistar rats weighing 300–450 g. Methods for general preparation have been described previously (see Holtzman *et al*. 2006). Under urethane general anaesthesia (1–1.5 g kg^{-1} I.P.) rats were fixed in a stereotaxic frame and crus II of the cerebellum was exposed. Single-unit recordings were made from neurones located in lobules Crus Ic/II a/b.

Recording

In all experiments, neuronal units were recorded in the first layer of the cerebellar cortex. The depth from the surface was less than 700 μm and crossing of Purkinje cell layers was carefully determined in each electrode track. Signals from the microelectrodes were amplified (gain × 1000–10000), filtered (band-pass 0.3–10 kHz) and digitised at 25 kHz. Some recordings were made using platinum–tungsten electrodes coated with quartz glass (80 μm shaft diameter, impedance 2–3 MΩ; Thomas Recording, Giessen, Germany) arranged in a 4 × 4 array (Eckhorn & Thomas, 1993), whilst on other occasions we used glass micropipettes pulled from filament glass broken to give tip impedances of 6–15 MΩ when filled with 0.5 M NaCl.

Extracellular recordings were made from a total of 91 Golgi cells, 51 of which were drawn from a previously published dataset (see Holtzman *et al*. 2006). These were identified using published criteria, including characteristic spontaneous firing patterns and significant long-lasting depressions in spike firing over a period of several hundred milliseconds, often accompanied by short-lasting excitations (SLEs) following stimulation of peripheral afferents: in previous studies, 19 neurones with these characteristics were labelled juxtacellularly and shown to be Golgi cells (Holtzman *et al*. 2006).

In this study, a total of 45 units were recorded which we classified as putative granule cells (for classification criteria see Supplmentary Fig. S2); in some cases double-unit recordings of granule cell and Golgi cell pairs on the same electrode ($n = 8$) were made possible by the superior recording characteristics of the Thomas recording electrodes.

Stimulation

Mixed low-threshold somatosensory afferents were stimulated using percutaneous pin electrodes inserted into the foot pads and vibrissal skin at rates generally <0.66 Hz (see Holtzman *et al.* 2006). In some experiments, parallel fibres were stimulated using surface electrodes (platinum–tungsten electrodes coated with quartz glass (Thomas Recording, Giessen, Germany); 80 μm shaft diameter, impedance 0.1 MΩ) that were positioned adjacent to the recording electrode (trains of 0.2 ms biphasic pulses, currents usually 100–200 μA, not exceeding 500 μA). Parallel fibre stimulation was used for antidromic spike activation in granule cells and to evoke glutamate release in order to activate mGluR2 receptors in Golgi cells.

Pharmcological agents and iontophoresis

For experiments involving iontophoretic drug delivery we manufactured electrodes incorporating a parylene-C-insulated stainless-steel recording electrode (2 MΩ, MPI Inc.) attached to theta glass capillaries (Clark capillaries, Harvard Instruments). Pipettes were broken to final tip diameters of 2–5 μm and then glued to the stainless-steel recording electrodes so that the steel recording tip protruded 50–80 μm beyond the capillaries. This arrangement allowed somatic recordings from Golgi cells in the first granular layer whilst biasing delivering drug some distance from the soma. Using theta capillaries allowed ionophoresis of drug and vehicle controls for the same Golgi cell. Holding currents of 20 nA were used for both drug and vehicle pipettes while searching for Golgi cells. Negative currents were applied independently to either barrel to eject either vehicle or negatively charged drugs (currents up to −20 nA). Pipette tip impedances were monitored throughout to ensure that blockage did not occur.

During the iontophoresis experiments, we used two highly selective mGluR2 receptor antagonists: LY341495 ($IC_{50} = 2.3$ nM) and (*RS*)-1-amino-5-phospho-noindan-1-carboxylic acid (APICA) ($IC_{50} = 30$ μM) (Tocris, UK). Pipette concentrations were 5 μM dissolved in 32 mM NaOH in dH_2O for LY341495, 1 mM in 44 mM NaOH in dH_2O for APICA. In other experiments the glycine receptor blocker strychnine ($IC_{50} = 20$ nM) was used: pipette concentration 1 mM dissolved in 0.9% w/v saline solution. These had different vehicles, which were controlled independently.

In other experiments, we used topical application of pharmacological agents including the selective mGluR2 receptor antagonist LY341495 (500 nM dissolved in 0.9% w/v saline solution) and the selective $GABA_A$ super-agonist 4,5,6,7-tetrahydroisoxazolo[5,4-c]pyridin-3-ol (THIP, Tocris UK; 100 nM dissolved in 0.9% w/v saline solution). Appropriate saline vehicle controls were performed in the same experiment prior to drug application. In all of these experiments, solutions were warmed to 37°C and only a single Golgi cell, isolated in the first granular layer, was tested in each cerebellar hemisphere so as to minimise drug contamination.

Spike train analysis

Spike trains were discriminated using a custom-written spike shape analysis and cluster-cutting package (LabSpike: available from http://www.pdn.cam.ac.uk/staff/dyball/labspike.html). Post-stimulus time histograms (PSTHs) were constructed from the time series (minimum 50 trials, usually >100) and quantified using cumulative sum (CUSUM) derivative analysis (Davey *et al.* 1986; Holtzman *et al.* 2006), which facilitates the detection of persistent changes in the histogram, that may not be visually apparent. CUSUMs were expressed relative to pre-stimulus firing levels, assessed over at least 200 ms, thus upward sloping portions of the CUSUM trend-line indicate increases in firing above pre-stimulus levels and vice versa, whereas a level CUSUM trend-line indicates no change in firing compared to pre-stimulus levels. Response onsets and offsets were measured using the turning points of the CUSUM trend-lines, as assessed by eye (see Fig. 5). The impact of drugs on Golgi cell responses was assessed by dividing the duration of the response into deciles (in order to normalise for differing response durations between cells) and comparing the firing rate depression in each decile relative to the pre-stimulus firing, based on samples of at least 100 stimuli before and after the drug application. Data for different Golgi cells were then grouped by decile and paired Student's *t* tests or Wilcoxon signed-rank tests were used, as appropriate, to assess the effects of the vehicle and drug within the group of tested cells. During these experiments, sensory stimuli (e.g. limb stimulation) were delivered continually at a rate not exceeding 0.66 Hz. We also assessed the stability of Golgi cell responses over the extended periods of time required to test drug effects (see Supplmentary Fig. S1).

Glutamate biosensors

In some experiments we used custom-built glutamate-sensitive biosensors to measure levels of extracellular

glutamate in the cerebellar cortex. Glutamate was detected amperometrically through the evolution of peroxide using enzyme-modified electrodes (fabrication and characterisation described in Frey *et al.* 2010). Briefly, 6-mm-shaft silicon microprobes (cross-section of 40 μm × 100 μm) were fabricated with two 10-μm-deep recessed Pt microelectrodes (surface area 50 μm × 150 μm) separated by 200 μm. An Ag–AgCl reference electrode (surface area 40 μm × 500 μm) was integrated on the same shaft. The Pt electrodes were modified to selectively detect glutamate: on the first electrode (glutamate sensing), glutamate oxidase was immobilised using electrochemically aided adsorption combined with chemical co-cross-linking with bovine serum albumin and the cross-linking agent glutaraldehyde. Interference from small, electroactive molecules present in the extracellular fluid, such as dopamine and ascorbic acid, was reduced with two procedures. Firstly, a second electrode (non-glutamate sensing) was also coated by a bovine serum albumin membrane that lacked the glutamate oxidase enzyme. Our measurements were performed in differential mode – signal from the non-sensing electrode was subtracted from the signal arising from the glutamate-sensing electrode. Secondly, we electropolymerised *m*-polyphenylenediamine, which acts as a permselective membrane, onto both electrodes. This substantially improved signal-to-noise ratios, thus allowing measurement of selective glutamate signals.

Prior to *in vivo* measurements, biosensors were calibrated in 0.01 M phosphate-buffered saline solution at room temperature and assessed for selectivity by increasing glutamate (10 μM increments), dopamine (2 μM) and ascorbic acid (200 μM) concentrations in the physiologically expected range. Example calibration measurements are shown in Fig. 2*D*, where the sensor is first tested with glutamate, followed by serial additions of further glutamate, dopamine, ascorbic acid and finally more glutamate. A 3-electrode set-up was used for calibration comprising a standard Ag–AgCl reference electrode and a Pt wire as counter electrode (supplied by Metrohm, Runcorn, UK). Biosensors with a sensitivity >5 pA μM^{-1}, a linear range >20 pA, a limit of detection <1 μM and an interference rejection of >95% were chosen for *in vivo* recordings. *In vivo* recordings were made using a 2-electrode configuration using the integrated (i.e. on-shaft) Ag–AgCl electrode as combined reference–counter electrode. Both working electrodes (i.e. glutamate- and non-glutamate-sensing electrodes) and the Ag–AgCl electrode were connected to a PalmSens bi-potentiostat (Palm Instruments BV, the Netherlands) applying a constant potential of ~0.7 V *vs.* Ag–AgCl. The current signal was sampled at 16 Hz (unfiltered).

Results

In this series of experiments, we have addressed the functional interplay between Golgi cells and granule cells using pharmacological manipulation of extra-synaptic receptors, direct measurement of extra-synaptic glutamate levels, cross-correlation analysis of spontaneous activity, comparison of receptive fields and response dynamics during sensory information processing.

mGluR2 receptors contribute to Golgi cell long-lasting depression responses

Most commonly, Golgi cells respond to sensory input from wide receptive fields with long-lasting firing rate depressions (Holtzman *et al.* 2006) during which we hypothesise that granule cells would show increased activity. Such activity is expected to cause a rise in extra-synaptic glutamate, necessary for the activation of inhibitory mGluR2 receptors leading to long-lasting hyperpolarisations in Golgi cells (Yamamoto *et al.* 1976; Watanabe & Nakanishi, 2003).

Blockade of mGluR2 by inotophoresis of the highly selective, highly potent mGluR2 antagonist LY341495, or an alternative antagonist, APICA, produced a robust attenuation of the long-lasting depressions of Golgi cell firing, in agreement with this prediction. Raw data shown in Fig. 1*A* and *B* show the attenuation of this response in an example Golgi cell (control, panel *A*; with LY341495, panel *B*). Post-stimulus time histograms (PSTHs) for this cell are plotted in Fig. 1*C*; pre-drug control, continuous line; drug, broken line. Figure 1*D* plots grouped data for 18 Golgi cells tested in the same way, showing that LY341495 produced a significant attenuation of the depression responses across deciles 3–10 ($P = 0.0415$, 0.0241, 0.0094, 0.0132, 0.0177, 0.0017, 0.0042 and 0.0020, respectively, indicated by *; Student's *t* test or Wilcoxon ranksum, as appropriate), by the amounts indicated in the bar chart (upper panel). Later phases of the response were attenuated to a greater extent than earlier phases, thus LY341495 shortened the duration of the evoked Golgi cell responses. In seven of these experiments, we used theta-glass capillaries, allowing iontophoretic application of vehicle in the same locus, prior to delivery of the drug during the same experiment. No significant changes in the long-lasting depression responses were detected across the sample of Golgi cells tested following vehicle delivery (Fig. 1*E*).

Although we cannot know for sure the effective drug concentrations achieved using *in vivo* iontophoresis, our pipette concentration of LY341495 (5 μM) is considerably lower than that used in other similar studies (25 mM in Cirone & Salt, 2001), and any ejected drug would be rapidly diluted in the extracellular space. The antagonist LY341495 is very specific but may still have affected mGluRs other than mGluR2. Therefore, we applied the

same protocols using an alternative mGluR2 antagonist, APICA. Golgi cell depressions were also attenuated by application of APICA in a similar way (Fig. 1*F*). Grouped data for 11 Golgi cells (Fig. 1*G*) showed significant attenuations of the evoked depressions across deciles 4–10 ($P = 0.0308$, 0.0199, 0.0126, 0.0126, 0.0056 and 0.0041, respectively, indicated by *; Student's *t* test or Wilcoxon ranksum, as appropriate) whereas the vehicle control data ($n = 10/11$; different vehicle from LY341395 – see Experimental procedures) showed no detectable change in the evoked depressions (Fig. 1*H*). Crucially, APICA has no significant effect on group I or III mGluRs at our pipette concentration (1 mM; Ma *et al.* 1997); thus, the observed suppression of Golgi cell responses by both APICA and LY341495 at these concentrations can only be attributed to mGluR2. Our findings suggest that mGluR2 underpins an important mechanism responsible for mediating long-lasting inhibition of Golgi cell activity during sensory information processing *in vivo*.

Alterations in glutamate levels affect Golgi cell behaviour

Inhibitory glutamatergic actions via mGluR2 could arise from mossy fibres and/or parallel fibres, both of which

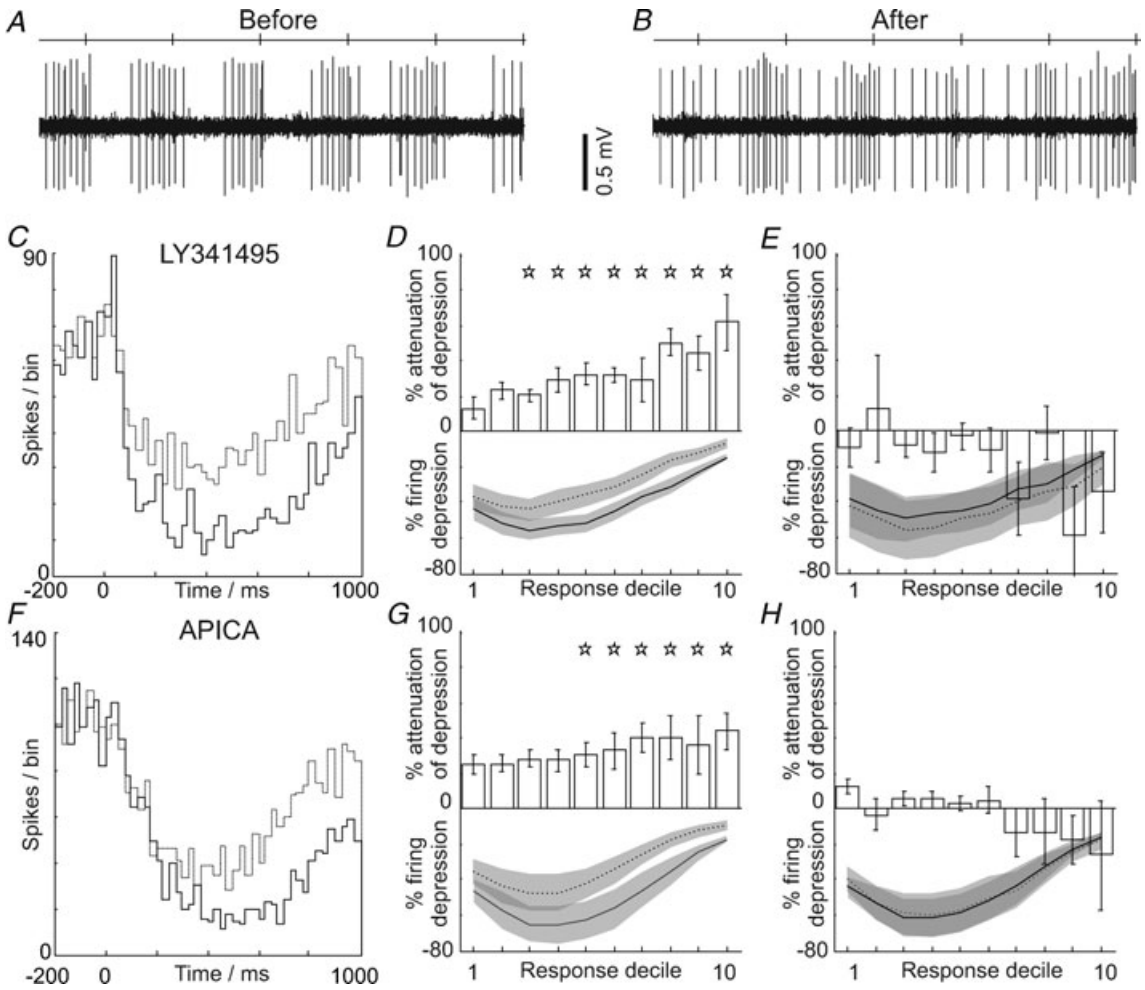

Figure 1. mGluR2 antagonism attenuates Golgi cell responses evoked by peripheral afferent stimulation
A and *B* show excerpts of raw data from an example Golgi cell during hindlimb stimulation (stimulus times indicated by ticks on the top line), before and during iontophoresis of LY341495. Note the attenuation of the evoked long-lasting depression response. The PSTHs shown in *C* summarise the data for the cell illustrated: before (continuous line) and after mGluR2 antagonism (broken line) with LY341495. Note the attenuation of the depression. *D* summarises grouped data ($n = 18$). The lower panel shows the normalised mean firing depression before (continuous line) and after mGluR2 blockade (broken line) – grey areas indicate 95% confidence intervals, error bars represent 2 standard errors from the mean. The upper panel shows the percentage attenuation of the response, with significant attenuation (indicated by stars) across deciles 3–10 of the responses; *E*, no significant changes in response occurred with vehicle administration. *F–H*, plot data in the same format as *C–E* for an alternative mGluR2 antagonist, APICA. *G*, shows grouped data for 11 cells.

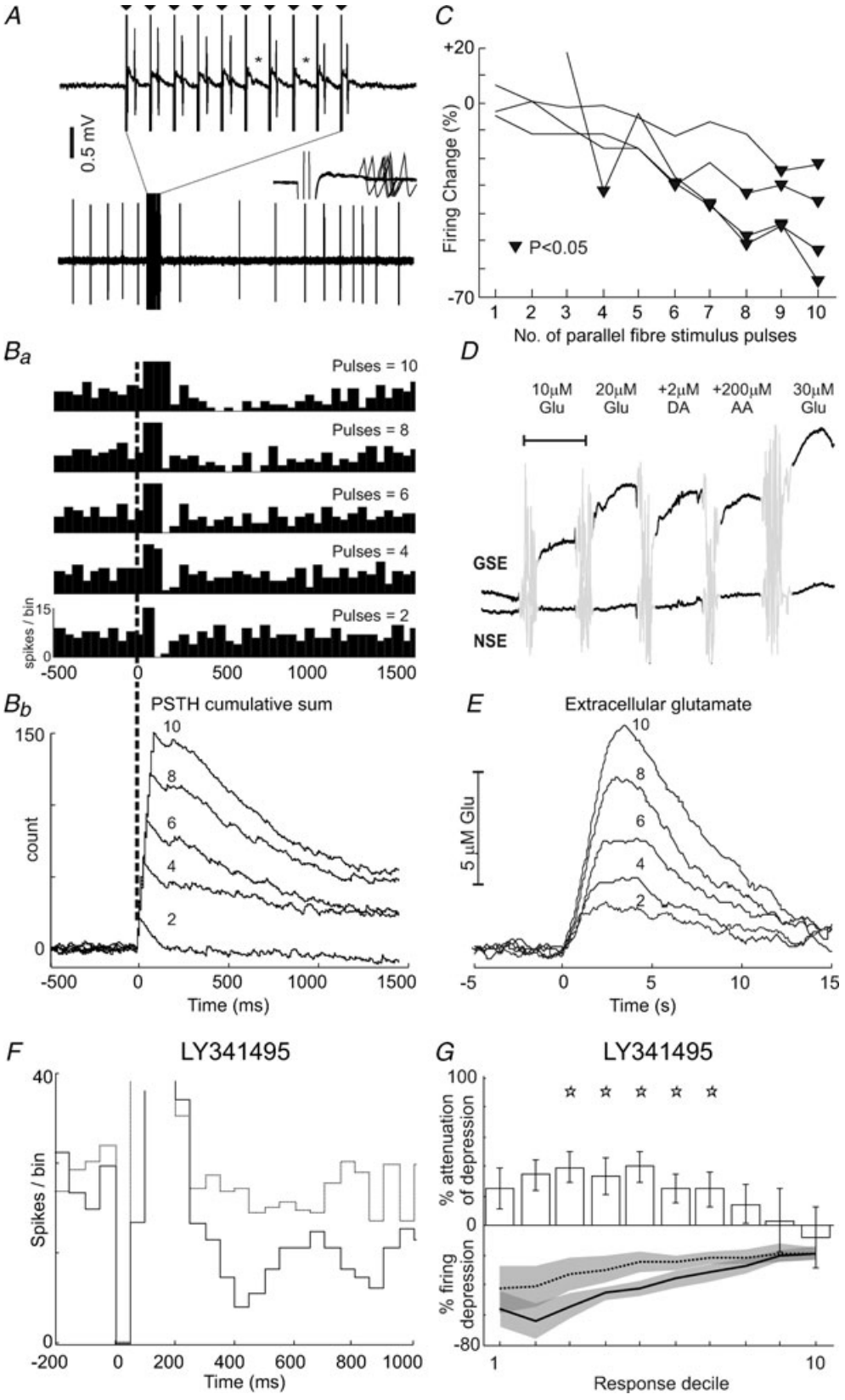

Figure 2. Direct parallel fibre stimulation inhibits Golgi cells via mGluR2
Raw data in *A* show a 2.5 s excerpt from an example Golgi cell recording during parallel fibre stimulation (10 pulses, 100 Hz). Note the prolonged depression of firing that follows the stimulus train. The stimulation period

innervate Golgi cells. We examined whether parallel fibre inputs could generate these responses in Golgi cells by directly stimulating parallel fibres combined with mGluR2 blockade. We also performed experiments using parallel fibre stimulation combined with amperometric measurement of spillover glutamate.

We used a stimulation protocol similar to that used in the *in vitro* slice preparation of Watanabe and Nakanishi (2003), to test eight Golgi cells with parallel fibre stimulation and topically applied mGluR2 antagonist. Raw data showing the response of a Golgi cell to parallel fibre stimulation are shown in Fig. 2*A*. Short-latency (∼3–4 ms, see inset) spikes were evoked by most stimuli in a train (10 pulses 100 Hz), although occasional 'failures' were also observed (6th and 8th stimuli marked by *), consistent with synaptic excitation via the parallel fibres. This behaviour was shown by 4/8 cells tested. Both these and the other four Golgi cells responded with prolonged firing rate depressions, which outlasted the parallel fibre stimulus train by hundreds of milliseconds (Fig. 2*A*, *Ba* and *F*). An example PSTH showing such a response (following the excitation; 250 ms onwards) is shown in Fig. 2*F*. Prolonged excitations outlasting the stimulus train, mediated via AMPA receptors (Watanabe & Nakanishi, 2003; their Fig. 6) were also seen in three of the cells that did not show short latency responses during the stimulus train (Fig. 2*F*; 100–250 ms). The remaining cells did not show appreciable excitations. The effects of varying the numbers of pulses in the stimulus train were systematically examined for four of the Golgi cells. Example PSTHs and CUSUMs (flat, same firing rate as pre-stimulus period; upward, firing above pre-stimulus levels and vice versa – see Experimental procedures) for the cell illustrated in Fig. 2*A* are shown in Fig. 2*Ba* and *Bb*. The increasingly shallow downward gradients of the CUSUMs indicate diminishing 'strength' of the prolonged depressions evoked with decreasing numbers of stimulus pulses, in tandem with weaker levels of excitation (initial upward deflection of the CUSUM), mirroring the findings of Watanabe & Nakanishi (2003). Normalising the depressions using the response to a train of 10 pulses as a 'standard', the degree of depression was calculated across the same time-window for decreasing numbers of parallel fibre pulses; grouped data are plotted in Fig. 2*C*. As expected, 'stronger' depressions arise from increasing pulse numbers, while low numbers of parallel fibre pulses (<4) failed or at best evoked weak depressions, suggesting that synchronised high-frequency parallel fibre activity is needed for activation of mGluR2 via spillover. Granule cells commonly respond to sensory input with short-lasting excitations, generally consisting of two to four spikes at instantaneous frequencies of ∼700 Hz as shown in Supplementary Fig. S4, comparable to other studies (Chadderton *et al*. 2004; Jorntell & Ekerot, 2006; Rancz *et al*. 2007). These bursts of high-frequency spiking would be expected to generate glutamate spillover, similar to our much lower frequency parallel fibre stimuli (6–10 pulses, 100 Hz).

We used glutamate-sensitive electrodes (biosensors) inserted into the molecular layer to assess glutamate spillover arising from the parallel fibre stimulation. Figure 2*D* shows *in vitro* calibration data recorded for an example probe in which signals from a glutamate-sensing electrode (GSE) and a non-sensing electrode (NSE; see Methods) are shown. Since the non-sensing electrode lacks glutamate oxidase, it showed no sensitivity to glutamate,

is expanded (upper records) to show individual stimulus artefacts (indicated by triangles, 10 ms intervals). Note the failure to evoke a short-latency spike (indicated by *) following pulses 6 and 8 of the train. Inset shows a 5 ms period following the same pulses – note the 'jitter' of the evoked spikes, indicating their synaptic origin. *Ba* and *Bb* illustrate PSTHs (15 trials for each case, bin-size 50ms; *y*-axes are truncated to focus on depression responses at the expense of early excitations) and CUSUMs (bin-size 5ms) of the response of the same Golgi cell to trains of 10, 8, 6, 4 and 2 parallel fibre stimuli at 100 Hz. The prolonged firing depressions diminish in 'strength' with decreasing numbers of stimuli, also indicated by the decreasing downward gradients in the CUSUMs. *C* shows grouped data for 4 different Golgi cells tested in the same way comparing the 'strength' of firing depression with number of stimuli. Triangles indicate points of significant firing depressions. *D* shows pre-implantation calibration data for a glutamate-sensitive electrode used to measure changes in ambient glutamate levels following parallel fibre stimulation. Only the glutamate-sensing electrode (GSE) is designed to sense glutamate; note the stepwise response to increasing glutamate (Glu) concentrations. Note the lack of response of the electrode lacking glutamate oxidase (NSE). Neither electrode responds to the electroactive species dopamine (DA) or ascorbic acid (AA). Scale bar, 100 s; mixing artefacts are greyed-out. *E*, data from the same glutamate-sensing electrode following local parallel fibre stimulation using the same stimulus protocols as for Golgi cells (superimposed numbers indicate stimulus train length). Mirroring the firing depressions in Golgi cells, peak levels of ambient glutamate decrease in line with shorter parallel fibre trains. *F*, PSTHs showing the responses of an example Golgi cell to parallel fibre stimulation (10 pulses, 100 Hz) before and after LY341495 application (continuous and dashed lines, respectively). In this example, stimulus artefacts (zero bins 0–90 ms) obscured recording during the train. Parallel fibre stimulation produces a pronounced excitation followed by a prolonged depression in firing (continuous line). Following application of LY341495 to block mGluR2, the prolonged depression was substantially attenuated (dashed line) – note that PSTH is scaled to optimise the evoked depression response. Grouped data for eight Golgi cells tested in this way are plotted in *G*, which shows significant attenuation of the evoked depression across deciles 3–7 (indicated by stars).

thus acting as a suitable control electrode for differential recording. The calibration measurements (Fig. 2*D*) show the glutamate-sensing electrode reliably sensed increases in glutamate concentration and both electrodes effectively rejected dopamine and ascorbic acid in the physiological concentration range.

Figure 2*E* shows data from the same probe tested *in vivo* using parallel fibre stimulation. The traces show the differentially recorded signals from the biosensor, with the glutamate-sensing electrode located 200–350 μm deep from the surface (note the biosensor electrode dimensions of 50 × 150 μm; thus, the molecular layer was preferentially targeted), each trace representing the average of two trials at each of 10, 8, 6, 4 and 2 parallel fibre pulses, respectively (100 Hz, 500 μA, 0.2 ms biphasic). Qualitatively similar i*n vivo* measurements were performed using five probes in three animals.

We next tested the effects of mGluR2 blockade on the prolonged depressions of Golgi cell firing evoked by parallel fibre stimulation. Like the peripherally evoked responses, topically applied LY341495 substantially attenuated the depressions. Example PSTHs are shown in Fig. 2*F* (before drug, continuous line; with drug, broken line). Grouped data for eight Golgi cells tested in this way are shown in Fig. 2*G*, showing that LY341495 (500 nM) significantly attenuated parallel fibre-evoked depressions across deciles 3–7 ($P = 0.0253$, 0.0177, 0.0281, 0.0348 and 0.0397, respectively, indicated by *; Student's *t* test or Wilcoxon ranksum, as appropriate). Parallel fibre-evoked excitations were unchanged following application of LY341395. At the applied concentration, LY341495 would not produce any significant action at Group I mGluRs (K_i/IC_{50} $mGlu_{1a} = 6800$ nM, K_i/IC_{50} $mGlu_{5a} = 8200$ nM, Ki = absolute inhibition constant) but nonetheless suppressed Golgi cell responses. LY341495 might have moderately blocked mGluR7 (K_i/$IC_{50} = 990$ nM) modulating P/Q-type Ca^{2+} channels, leading to decreased granule cell synaptic transmission (Perroy *et al.* 2000). However, we consider it most likely that LY341495 directly blocked Golgi cell mGluR2 receptors, accounting for the suppression of parallel fibre-evoked depressions in these cells.

These experiments show that high-frequency (>4 pulses at 100 Hz) parallel fibre stimulation leads to micromolar level increases in spillover glutamate *in vivo*, and that these concentrations are necessary and sufficient for activation of mGluR2-mediated inhibition in Golgi cells.

Selective inhibition of granule cells alters Golgi cell behaviour

As we show *in vivo* in the present study and others have shown *in vitro* (Watanabe & Nakanishi, 2003), parallel fibre stimulation can release sufficient glutamate to *inhibit* Golgi cells. Since mGluR2 receptors are not linked to synaptic structures, but are freely mobile (Lujan *et al.* 1997), mossy fibres might also contribute inhibitory glutamate directly (Mitchell & Silver, 2000*a*) following somatosensory activation. To address this issue, we exploited the specific α6- and δ-subunit-containing $GABA_A$ receptors which are expressed exclusively at extra-synaptic locations on granule cell dendrites within the cerebellar cortex (Brickley *et al.* 1996; Rossi & Hamann, 1998). Selective inhibition of granule cells using THIP, a super-agonist at these receptors (Mortensen *et al.* 2004, 2010; Storustovu & Ebert, 2006) allowed us to assess the potential contribution of granule cell-derived inhibitory glutamate to Golgi cell responses, without affecting direct mossy fibre inputs. Topically applied THIP reliably attenuated the evoked depression in the Golgi cells; example PSTHs are shown in Fig. 3*A*. A total of 10 Golgi cells were tested with THIP; group

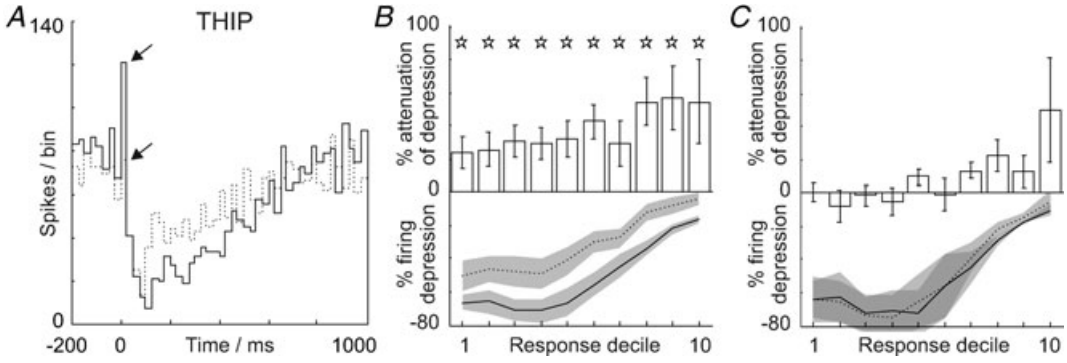

Figure 3. Selective inhibition of granule cells attenuates Golgi cell responses
A–C demonstrate the effects of generating strong tonic inhibition in granule cells, using a $GABA_A$ super-agonist, THIP. *A*, application of THIP attenuates both the short-lasting excitation (highest bin indicated by upper arrow, cf. lower arrow) and the ensuing long-lasting depression response of the Golgi cell to limb afferent stimulation. *B*, grouped data ($n = 10$) showing a significant response attenuation across all response deciles (indicated by stars) and *C*, absence of vehicle (saline) effects.

data are presented in Fig. 3*B*, which shows significant attenuations in all response deciles ($P = 0.0233$, 0.0128, 0.0067, 0.0081, 0.0047, 0.0020, 0.0118, 0.0004, 0.0035 and 0.0031, respectively, indicated by *; Student's *t* test or Wilcoxon ranksum test, as appropriate). Topically applied saline vehicle control data ($n = 4/10$ cells tested; vehicle applied in the same experiment prior to THIP) are shown in Fig. 3*C*. Note also in this example PSTH, the Golgi cell response includes an initial excitation (highest bin indicated by arrow and continuous line in *A*) which was also sensitive to THIP (cf. dashed line). Across our sample tested with THIP, 6/10 Golgi cells had short-lasting excitation responses of this type (all limb evoked; trigeminal excitations not tested) and 3/6 of these were attenuated by THIP ($P < 0.02$, Fisher-exact tests based on highest bin value (latency < 25 ms) within the period defined by the control response, see Fig. 3*A*) whilst the excitation of the remaining three neurones were unaffected, despite significant attenuation of their depression responses. This suggests that the limb-evoked excitations in our Golgi cells may have been mediated in part by underlying granule cell excitation (THIP sensitive) and in part by direct mossy fibre inputs (Holtzman *et al.* 2009).

Although acting through a very different mechanism, reducing granule cell excitability using THIP mirrors the effects of direct blockade of mGluR2. We conclude, therefore, that granule cells are an important source of inhibitory glutamate responsible for suppressing Golgi cell activity during sensory information processing.

Interrelated activity of granule cells and Golgi cells

Our data imply that granule cells may have a substantial *inhibitory* role with respect to Golgi cells. We examined the inter-relationships between Golgi cells and granule cells (classified using a range of criteria, detailed in Supplementary Fig. S2) by analysis of their spontaneous activities and, in particular, considering our data with THIP indicating that granule cells are an important source of inhibitory glutamate, we sought evidence that granule cell response patterns might be timed appropriately so as to provide inhibitory glutamate during the Golgi cell depression responses.

Spontaneous activity. Cross-correlation analysis was performed using spontaneous activity from three double-unit recordings of Golgi cells and putative granule cells (recorded simultaneously on the same electrode). In two of these cases, high-frequency 'bursty' activity in granule cells *preceded* prolonged depressions of Golgi cell activity. This type of activity is a common feature of granule cells (Chadderton *et al.* 2004; Jorntell & Ekerot, 2006) and it may be well suited to evoke increases in glutamate levels. Figure 4*A* shows 3 s of raw data from one of these double-unit recordings of a Golgi cell (for classicification see Holtzman *et al.* 2006) and putative granule cell on the same electrode. The expanded section shows the smaller amplitude spikes of the granule cell. Long silent periods are interspersed with erratic activity that includes very short intervals (2–3 ms, 300–500 Hz). Similar data from a different Golgi–granule cell pair is shown in Fig. 4*B*. We consider it is probable that such closely located cells (single-electrode pairs) may be linked with one another synaptically and, given that the Golgi cells showed depression responses, general correlations between pairs may be similar. Synchronous or short-latency coupling (i.e. peaks or troughs near zero lag) was absent, although when considered on broader time scales 2/3 pairs showed robust relationships in their firing patterns (illustrated in Fig. 4*A* and *B*). The cross-correlograms for these two pairs are illustrated in Fig. 4*C* and *D*, which plots Golgi cell activity with respect to granule cell spikes. In both cases, Golgi cell firing was significantly depressed for several hundred milliseconds following granule cell spikes (which tended to occur in bursts), also evident in the raw data shown. Although limited in terms of cell pairs (in 5 other Golgi–granule pairs, low levels of spontaneous activity in the granule cells precluded cross-correlation analysis), surprisingly, increased granule cell activity may correlate with *decreased* Golgi cell activity. This effect might be underpinned by mGluR2 activation arising from the high-frequency 'bursty' firing patterns of granule cells giving rise to increased glutamate levels (cf. Fig. 2*Ba* and *C*).

Evoked granule cell responses. Granule cell responses were classified into four latency-based categories (see Figs 5 and 6; detailed analysis of granule cell responses is given in Supplementary Fig. S3); early onset depressions (onset ~20 ms, duration 100–120 ms), late onset long-lasting depressions (onset >400 ms, duration ~500 ms), brief-lived short-latency short-lasting excitations (onset 5–20 ms, duration typically a few spikes) and long-latency long-lasting excitations (onset ~110–150 ms, duration several hundred milliseconds). For comparison alongside granule cell responses, we reproduce our earlier data on Golgi cell responses (see Holtzman *et al.* 2006).

Across a sample of 25 granule cells tested for responses from six standard peripheral areas (trigeminal and distal limbs), all showed long-lasting excitations from one or more inputs, suggesting that these responses are very common amongst granule cells. Figure 5*A* shows the responses of a double-unit Golgi–granule pair (same electrode) following single-pulse stimulation of ipsilateral forelimb afferents. In this example, the Golgi cell (top) shows the commonly evoked long-lasting depression

(LLD) response; correlated with this, the granule cell (bottom) shows a long-lasting excitation (LLE). The CUSUMs shown in Fig. 5*B* plot the onset latencies and firing trends of these responses (Golgi LLD, 45 ms, dotted line; granule LLE, 80 ms). Given the common occurrence of these long-lasting granule cell responses (and the considerable receptive field overlap – discussed next), populations of granule cells responding in a similar way could bring about dramatic increases in glutamate levels; thus, these response patterns may be ideally suited for driving mGluR2-mediated inhibition in Golgi cells.

Trigeminal stimulation evoked granule cell long-lasting excitations more commonly than corresponding long-lasting depressions in Golgi cells (indicated by * in Fig. 6*A*; $P < 0.01$ Fisher exact test), whereas these responses were evoked with equal likelihood from each of the limbs. Onset latencies for these granule cell long-lasting excitations were on average approximately 100 ms later than the Golgi cell depressions (indicated by * in Fig. 6*B*, Students *t* test or Wilcoxon ranksum test as appropriate, $P < 0.001$), giving an 'average' onset latency of ∼110–150 ms. The offsets of granule cell and

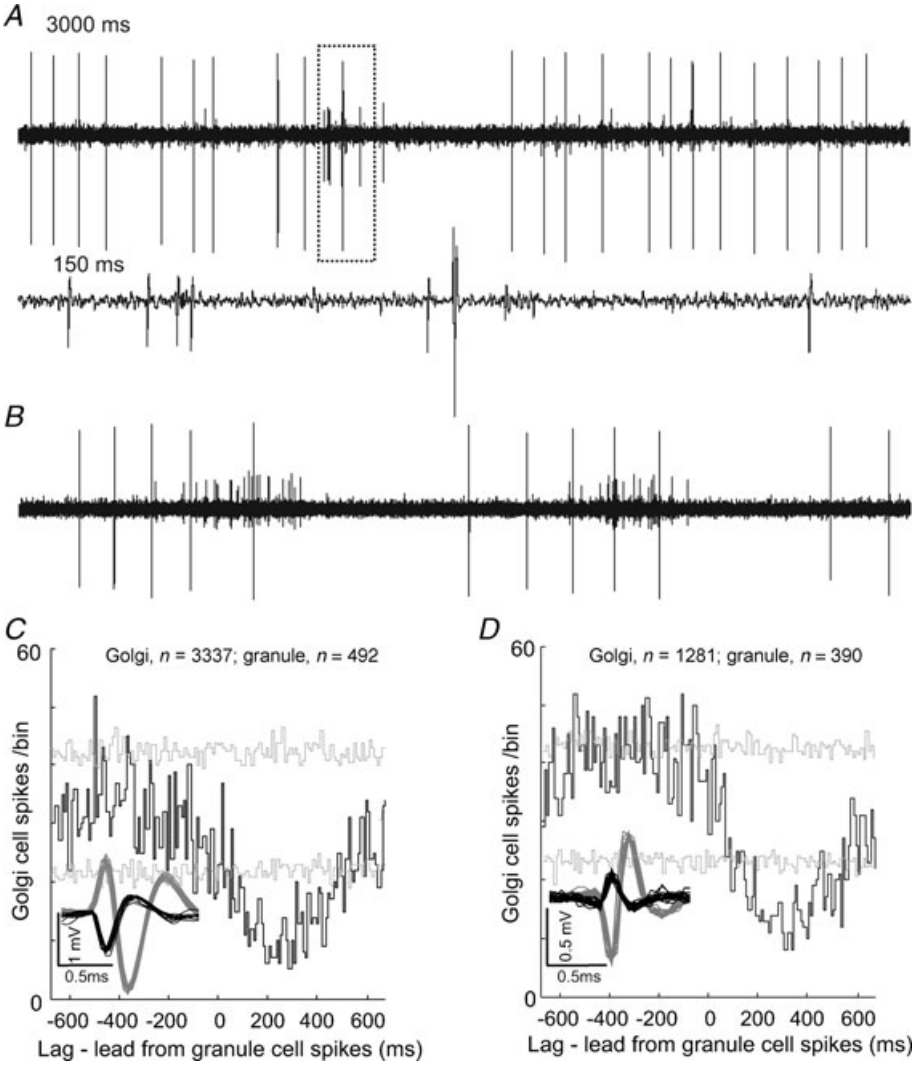

Figure 4. Cross-correlation analysis of Golgi–granule cell pairs
A shows a 3 s excerpt of raw data from a double-unit recording of a Golgi cell (large spikes) and a granule cell. Notice the irregular activity pattern of the granule cell, particularly evident in the expanded section (dotted box and lower trace), representing 150 ms of data. Similar raw data for a different Golgi cell–granule cell pair are drawn in *B*. The cross-correlograms shown in *C* and *D* are derived from the paired recordings shown in *A* and *B*, respectively (bin-size 10 ms), and each plots Golgi cell activity with respect to granule cell spiking (numbers of spikes used from each cell indicated above each correlogram). Broken grey lines represent 95% confidence interval for the 'shift predictor' (calculated using 100 iterations of randomised spike train time-shifts). Note the significant ($P < 0.05$, i.e. cross-correlation bins exceeding the 'shift predictor' confidence interval) depressions in Golgi cell firing that follow granule cell spiking which are also evident in the selected raw data shown in *A* and *B*.

Golgi cell responses were closely matched showing no significant differences across inputs, except for ipsilateral trigeminal inputs (indicated by * in Fig. 6*B*, Students *t* test, $P < 0.01$). Overall, these findings suggest that these two cell types have overlapping receptive fields and there exists a close correlation between the dynamics of evoked long-lasting responses in Golgi cells and granule cells.

In addition to the prolonged excitations, granule cell responses also included short-lasting excitations and periods of depressed firing occurring before and/or after excitation responses. Figure 5*C* shows the responses of two simultaneously recorded granule cells (different electrodes ~400 μm apart, trigeminal stimulus). The first cell (top) shows both short-lasting (indicated by arrow) and prolonged excitations (20 ms and 200 ms), whereas the neurone illustrated in the lower PSTH shows only a prolonged excitation. Both neurones also show early periods of depressed firing (20–150 ms; preceding the long excitations) and later depressions (>400 ms onset). These response patterns are best seen from the CUSUMs in Fig. 5*D* (upward and downward triangles indicating prolonged excitations onset and offset/late depression onset, respectively). In some trials (12/62) the short-lasting excitation shown in the upper PSTH 'failed' but the early depression appeared nonetheless, whereas the early depression of the neurone shown in the lower PSTH occurred *without* preceding excitation. Across our sample, 90% and 40% of short-lasting excitations evoked from *ipsilateral* and *contralateral* trigeminal inputs, respectively, were accompanied by early depressions, suggesting that early depressions are unlikely to reflect post-excitation refractory periods; rather they represent independent inhibitory process(es). In the example shown, both granule cells also show late depressions (downward triangles in Fig. 5*D*), which were also observed in other granule cells following stimulation of limb inputs.

Golgi cells show brief but well-timed excitations (at similar latencies to granule cells, see Supplementary Fig. S4), that are ideally suited to increase phasic inhibition in granule cells giving rise to early depressions (Vos *et al*.

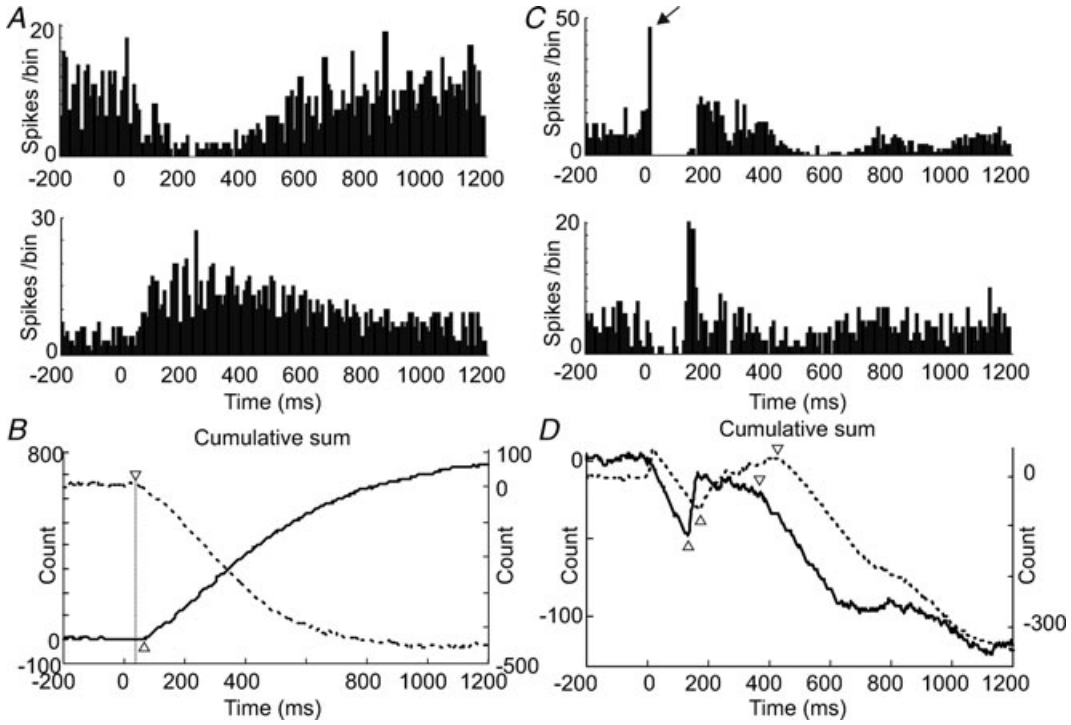

Figure 5. Comparison of the responses of Golgi cells and granule cells to sensory afferent stimulation
A shows PSTHs (bin-size 10 ms) for a Golgi cell–granule cell pair following stimulation of ipsilateral hindlimb afferents. The Golgi cell (upper panel) shows a typical long-lasting depression (LLD), whilst the granule cell shows a delayed onset long-lasting excitation (LLE). The CUSUMs in *B* show more clearly the time-course of these responses (Golgi cell, dashed line); triangles indicate onset latencies. The PSTHs (bin-size 10 ms) shown in *C* plot data from two simultaneously recorded granule cells (different electrodes) following stimulation of contralateral trigeminal inputs. In these examples, the cell in the upper panel shows both early (indicated by arrow) and late excitations (SLE and LLE), whereas the cell in the lower panel shows an LLE without SLE. The responses of both cells are interspersed with periods of early and late depression below spontaneous firing levels, seen more clearly as downward deflections in the CUSUMs plotted in *D* (upper cell, dashed line). Downward trends in the lines represent periods of reduced firing, relative to pre-stimulus levels; LLE onsets and offsets are indicated by upward and downward facing triangles, respectively.

1999; Holtzman *et al*. 2006; Crowley *et al*. 2009). Such responses could be evoked by any of the six standard inputs tested (Fig. 6*C*). Onset latencies and durations for early depressions are plotted in Fig. 6*D*. Early depressions of granule cell firing were more common from trigeminal inputs compared to the Golgi cell excitations (Fisher-exact tests, $P < 0.01$ ipsilateral, $P < 0.05$ contralateral). Overall, Golgi cell excitation responses (from any input) were

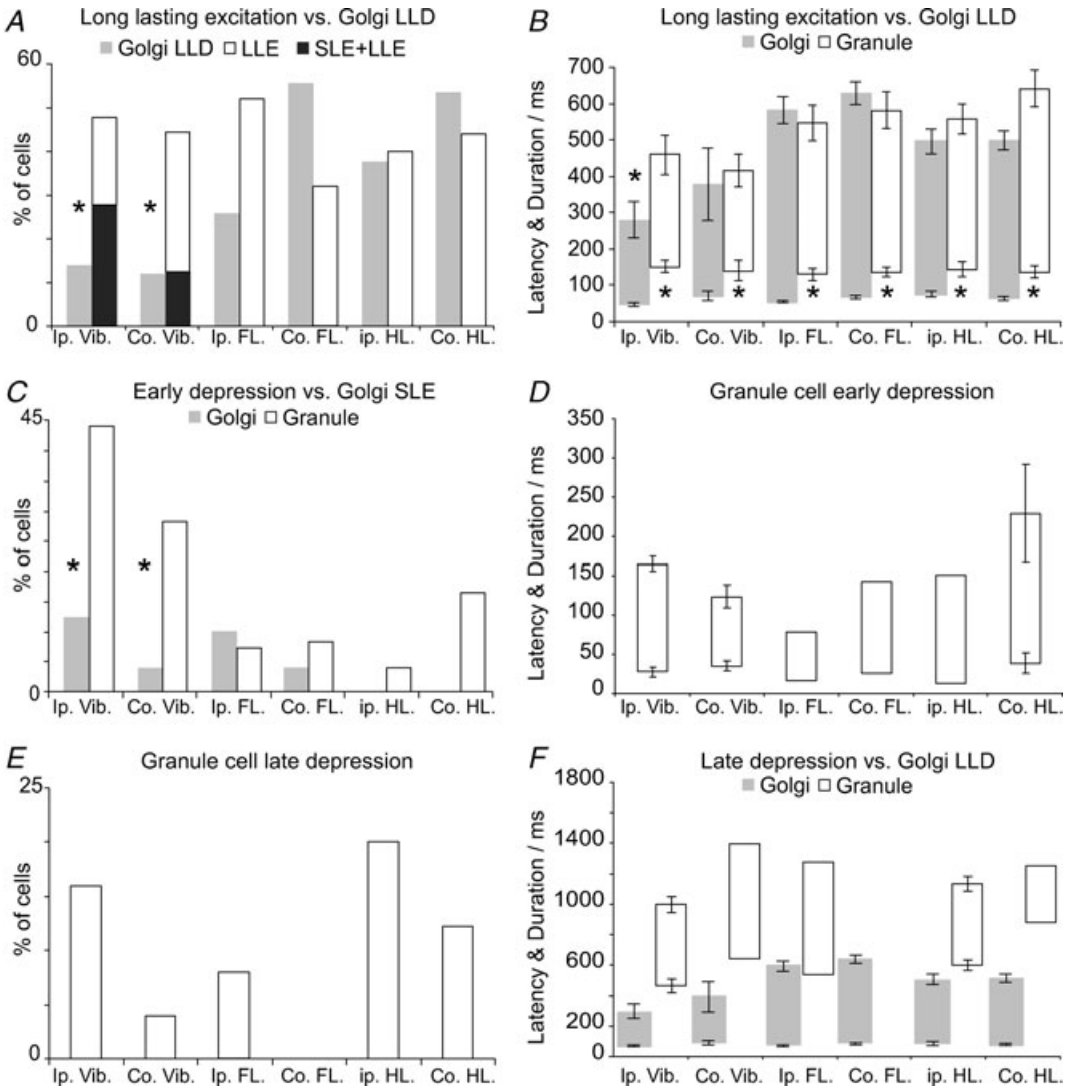

Figure 6. Comparison of response frequencies, onset and offset latencies in Golgi and granule cells
A, comparison of the likelihoods of Golgi cell long-lasting depression (LLD) responses relative to granule cell long-lasting excitation (LLE) responses (with/without SLEs, black and open bars, respectively). Granule cell LLE responses were significantly more frequently evoked from either side of the face compared to Golgi cell LLD responses, although no differences were found comparing limb responses. *B* shows a comparison of onset latencies and durations, revealing that the onsets of granule cell LLEs lag those of the Golgi cell LLDs by ∼100 ms, irrespective of the stimulus. Only ipsilateral trigeminal responses showed a significant difference in offset time. *C* plots the likelihood of granule cell early depressions against SLEs in Golgi cells. Early depressions were significantly more likely in granule cells than Golgi cell SLEs, which may mediate them. Although the sample of 51 Golgi cells used for this analysis did not include any with hindlimb evoked SLEs, such responses are seen in some Golgi cells in this region (see Holtzman *et al*. 2006). *D* plots onset latencies and durations for early granule cell depressions. *E* shows the occurrence of late inhibitions in our sample of granule cells (potentially underestimated due to low spontaneous firing rates). *F* re-plots the Golgi cell LLD data shown in *D* alongside comparable data for granule cell late inhibitions. Late depressions evoked from the contralateral forelimb were seen in other granule cells not included in the receptive field dataset. A relatively small sample size precludes statistical analysis, although late inhibitions appear to correlate with offset of Golgi cell LLDs, i.e. the restoration of Golgi cell firing. In all cases error bars represent 2 standard errors from the mean; no error bars for samples $n < 4$. Abbreviations: Ip., ipsilateral; Co., contralateral; Vib., Vibrissal skin; FL., forelimb; HL., hindlimb

evoked in 13/51 neurones (25%, see Fig. 6*C*, grey bars), whereas granule cell early depressions, from any input, were more frequent 12/25 cells (48%, Fig. 6*C*, open bars), a difference that was significant ($P < 0.02$, Fisher-exact test). The mismatch between the likelihood of granule cell early depressions and Golgi cell excitations is consistent with a degree of synaptic divergence between inhibitory Golgi cell synapses and their granule cell targets (Jakab & Hamori, 1988; Crowley *et al*. 2009).

Late depressions of activity in granule cells were observed in 9/25 cells (36%) from a variety of inputs (Fig. 6*E*). Onsets and durations are plotted in Fig. 6*F*, alongside the Golgi cell depression data. These data suggest that late depressions coincide with the recovery of Golgi cell firing following prolonged depressions (cf. Figs 5*A* and *C*, and 8*A*), suggesting that granule cell excitations are curtailed by a resumption of Golgi cell activity.

Gycinergic inhibition in Golgi cells

In vitro studies have shown that Golgi cells receive glycinergic inhibition exclusively from Lugaro cells (Dumoulin *et al*. 2001). To address the possibility that this mechanism contributes to the long-lasting depressions of Golgi cell firing, we used *in vivo* iontophoresis of strychnine to block these receptors. We observed robust attenuation of Golgi cell depressions after blockade of glycine receptors. PSTHs for an example neurone are plotted in Fig. 7*A* (control, continuous line; drug, broken line). Grouped data for 14 Golgi cells tested with strychnine are plotted in Fig. 7*B*. Strychnine significantly attenuated the evoked depressions in deciles 6–10 ($P = 0.0495$, 0.0057, 0.0058, 0.0068, 0.0100 and 0.0085, respectively, indicated by *; Student's *t* test or Wilcoxon ranksum, as appropriate). Strychnine was dissolved in 0.9% saline; vehicle control data for topically applied saline are shown in Fig. 3*C*. We cannot be sure of the effective concentration of strychnine achieved in the tissue using *in vivo* iontophoresis, although our pipette concentration (1 mM) is substantially lower than that used in other investigations (10–20 mM; Gai & Carney, 2008; Sanchez *et al*. 2008; Iwamoto *et al*. 2009; Kutscher & Covey, 2009). The responses of a representative Lugaro cell under similar conditions are shown in Supplementary Fig. S6 – note the prolonged increase in spiking over 300–600 ms in agreement with the findings of other investigators (Van Welie & Hausser, 2009). Our data suggest that glycinergic inhibition, mediated by Lugaro cells, plays an important role in suppressing Golgi cell activity during sensory information processing, alongside granule cell-driven mGluR2 inhibition.

Relationship of Golgi and granule cell activity to Purkinje cell activity

The patterns of granule cell activity we describe here, in addition to exciting and, in particular, being well suited to inhibit Golgi cells, will also excite other cortical neurones. Our prior work, using the same preparation, described subtle but prolonged simple spike excitations in Purkinje cells (see Holtzman *et al*. 2006). Figure 8*A* shows the responses from an ensemble simultaneous recording including a Golgi–granule cell pair (same electrode) with a Purkinje cell located ~600 μm distant medio-laterally. For clarity, the responses are drawn as CUSUM trendlines (cf. Fig. 5). In this example, the Golgi cell shows a depression response (light grey line; onset ~50 ms) and the granule cell shows long-lasting excitation (dashed line, onset >100 ms), preceding a later depression. The Purkinje cell (dark grey line) shows a delayed-onset simple-spike excitation. In Fig. 8*B* we re-plot the data from Fig. 5*D* alongside comparable data for Purkinje cell simple-spike excitation responses derived from a sample of 76 Purkinje cells (previously published in Holtzman *et al*. 2006). Overall, Golgi cell depressions start earlier than Purkinje cell responses (indicated by *; $P < 0.01$, Student's *t* test or Wilcoxon ranksum test, as appropriate, except contralateral forelimb). In contrast, Purkinje cell simple-spike responses start at approximately the same time as granule cell long-lasting excitations (except contralateral forelimb). Purkinje cell response durations/offsets outlasted both Golgi cell and granule cell responses (indicated by †, $P < 0.03$ for Golgi cells, $P < 0.01$ for

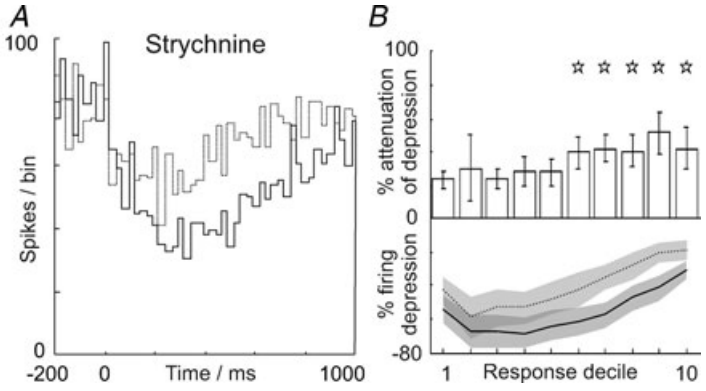

Figure 7. Antagonising glycinergic transmission attenuates Golgi cell responses evoked by peripheral afferent stimulation
A and *B* plot data testing the effects of blocking glycinergic inhibition in Golgi cells, using the glycine receptor antagonist strychnine. The PSTHs shown in *A* summarise the responses of an example Golgi cell before (continuous line) and after iontophoresis of strychnine (broken line). Grouped data are shown in *B* ($n = 14$) following the same format as Fig. 1*D* and *G*; significant attenuations were seen across response deciles 6–10 ($P < 0.05$).

granule cells). These observations indicate that in addition to inhibiting Golgi cells during the depression responses, granule cell long-lasting excitations also drive Purkinje cell simple-spike responses, although Purkinje cell activity tends to outlast that of granule cells by 300–500 ms.

Discussion

Golgi cell behaviour

Our experiments reveal a complex functional interplay between Golgi cells and granule cells and highlight the importance of glutamatergic and GABAergic transmission in regulating prolonged activity in these functional loops. Granule cell-derived glutamate provides predominant *inhibition* to Golgi cells (via mGluR2 receptors) which is counteracted by spillover of Golgi cell GABA onto granule cells. These mechanisms may be supplemented by glycinergic inhibition of Golgi cells supplied by Lugaro cells (see Dumoulin *et al.* 2001). Prolonged periods of depressed firing (below their ongoing spontaneous levels) have been observed in Golgi cells during information processing *in vivo* in a variety of species (Edgley & Lidierth, 1987; Vos *et al.* 1999; Barmack & Yakhnitsa, 2008; Prsa *et al.* 2009) suggesting that our results represent a generalised form of Golgi cell behaviour.

Artificially elevating glutamate levels, using parallel fibre stimulation resembling 'bursty' granule cell firing (1–10 pulses at 100 Hz), evoked excitations and prolonged inhibitions which commonly appear hand-in-hand in Golgi cells, in close agreement with Watanabe and Nakanishi (2003). However, when using somatosensory stimulation, excitations are much rarer and inhibition alone dominates (see Fig. 6*A* and *C*, and Holtzman *et al.* 2006) suggesting that glutamate can be purely inhibitory to Golgi cells. Indeed, Yamamoto *et al* (1976) demonstrated a depression of Golgi cell firing to bath-applied glutamate *in vitro,* compared to excitation of other cerebellar cortical neurones. The inhibition was non-GABAergic, non-glycinergic, and persisted in tetrodotoxin, so was not mediated by cortical interneurones (see their Figs 1 and 2).

In Golgi cells, mGluR2 receptors are expressed throughout the cell and are not localised to any particular

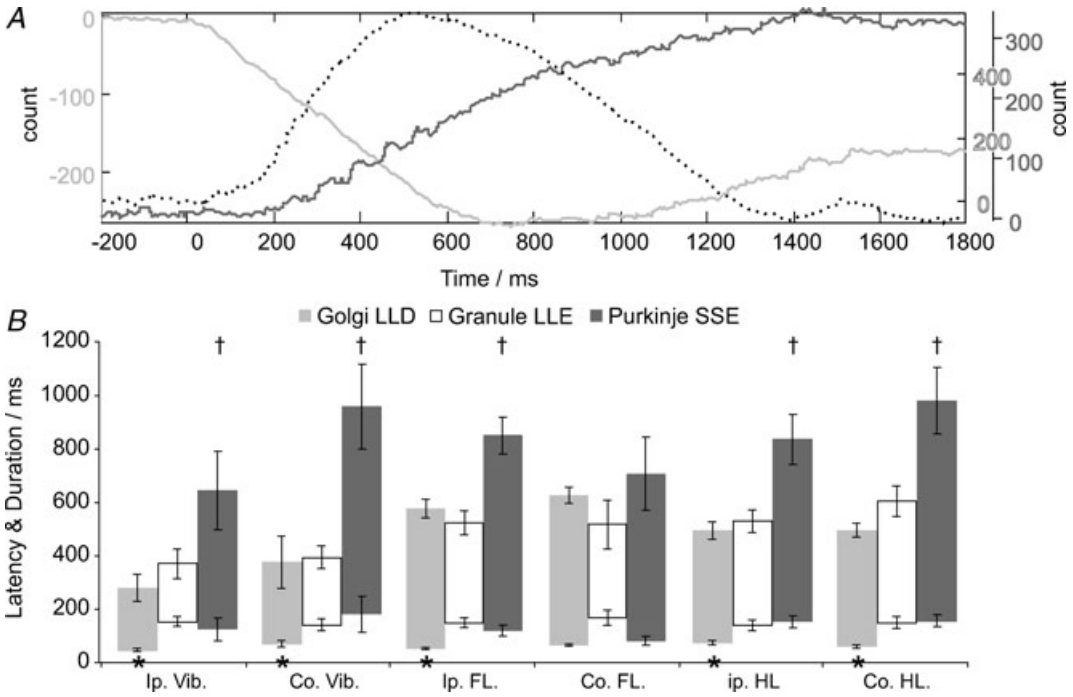

Figure 8. Relationship of Golgi and granule cell activity to Purkinje cell firing
The CUSUMs plotted in *A* show the combined responses from a simultaneous ensemble recording involving a Golgi–granule pair and Purkinje cell ~600 μm away, following stimulation of ipsilateral hindlimb afferents. In this example, the Golgi cell (light grey line) shows a long-lasting depression (downward portion of CUSUM) correlated with a long-lasting excitation in the granule cell (broken line) which coincides with an increase in Purkinje cell simple spike activity (dark grey line). *B* plots population data comparing the Golgi cell depressions, granule cell excitations (already shown in Fig. 6*D*) against comparable data for Purkinje cell simple spike responses, showing the close relationship between granule cell activity and Purkinje cell simple spike responses, which were preceded by the earlier onset of Golgi cell depressions (indicated by *). Across the population, Purkinje cell responses tended to outlast those of Golgi cells and granule cells, indicated by †. Error bars represent 2 standard errors from the mean.

domain (Lujan *et al*. 1997) so they may be able to operate both pre- and post-synaptically as well as extra-synaptically. Our biosensor measurements confirm that parallel fibre stimulation sufficient to inhibit Golgi cells via mGluR2 activation generates increases in levels of extra-synaptic glutamate. Nonetheless, this does not prove that extra-synaptic transmission underpins the effects we observed. However, given the mobile nature of mGluR2 receptors, high-frequency 'bursty' firing (see Figs 4, S4 and 5), a common feature in granule cells (Chadderton *et al*. 2004; Bengtsson & Jorntell, 2009), may be ideally suited to mGluR2 activation. Individual granule cells are unlikely to contribute substantially to spillover glutamate, suggesting a further requirement for many granule cells to co-modulate periods of increased firing (see Fig. 5*C*) – a general necessity for Purkinje cell activation (Barbour, 1993) due to the considerable divergence between mossy fibres and granule cells (∼1:50; Jakab & Hamori, 1988). Such a threshold may act as a high-pass filter ensuring only relevant events trigger substantial glutamate spillover (Mitchell & Silver, 2000*a*,*b*) facilitating depression of Golgi cell activity.

A key strength of our experiments lies in the selectivity of the drugs we used and the Golgi cell-specific expression of extra-synaptic mGluR2/3 (rats: Ohishi *et al*. 1994) and glycine receptors (Dumoulin *et al*. 2001), and in the granule cell-specific expression of extra-synaptic δ-subunit containing $GABA_A$ receptors. Although unipolar brush cells (UBCs) also express mGluR2 and glycine receptors (Jaarsma *et al*. 1998; Dugue *et al*. 2005), they are rarest/absent in Crus II (where our recordings were made; see Dino *et al*. 1999). Moreover, dis-inhibition of UBCs by mGluR2 and/or glycinergic blockade would generate increased spillover glutamate which our study suggests would enhance Golgi cell depressions. In contrast, we only observed suppressions of these responses. Furthermore, antagonism of group I mGluRs would have been substantially lower than group II mGluRs in our experiments, so is unlikely to have contributed to the results; IC_{50} values for LY341495 are 6.8 μM for mGluR1 and 8.2 μM for mGluR5 (cf. 500 nM used in our parallel fibre experiments and IC_{50} 2.3 nM for mGluR2: Kingston *et al*. 1998) whilst APICA has no significant action at group I mGluR receptors up to 1 mM (Ma *et al*. 1997).

Despite prolonged excitations in granule cells, Golgi cell excitations are only brief-lived and relatively uncommon. Spiking in Golgi cells can inhibit neighbouring Golgi cells via gap-junction transmission of spike-after-hyperpolarisations (Dugue *et al*. 2009; Vervaeke *et al*. 2010), although our results suggest that further inhibition from slow mGluR2 and glycinergic IPSPs could also propagate across the Golgi cell network via gap-junctions. Golgi cell excitations may produce accurately timed phasic inhibition in granule cells (perhaps evident as granule cell early depression responses; cf. Jorntell & Ekerot, 2006, see Fig. 2 therein) thereby opposing mossy fibre drive to granule cells, possibly producing 'time-windowing' effects (see D'Angelo & De Zeeuw, 2009). However, it is unlikely that all granule cells will be equally affected on a short timescale, since ∼60% receive direct synaptic input from Golgi cells (Jakab & Hamori, 1988), whilst the remainder may 'sense' increases in glomerular GABA using 'slow' spillover mechanisms (Crowley *et al*. 2009).

Granule cell behaviour

Our study highlights the complex nature of granule cell excitations and inhibitions and their close relationship to changes in Golgi cell activity. Granule cells showed a prolonged excitation from one or more skin areas, in contrast to other investigations in the same region which only studied short-lasting excitations from focal receptive fields (Shambes *et al*. 1978; Chadderton *et al*. 2004; Rancz *et al*. 2007). Prolonged excitations resembling those we describe here have also been reported in cats by Eccles *et al*. (1971) and more recently by Jorntell and Ekerot (2006). In addition, periods of reduced firing were observed resembling early depressions (without preceding excitations – see Eccles' Figs 7–10; cf. Fig. 5*C* and Jorntell's Fig. 2) suggesting our data represent a generalised form of granule cell behaviour.

A fractured mosaic of mossy fibre representation dominated by ipsilateral trigeminal dermatomes has been reported for Crus II (80% lobular area corresponding to ipsilateral inputs; Shambes *et al*. 1978) leading other studies to focus on granule cell activation using ipsilateral trigeminal inputs (Chadderton *et al*. 2004; Rancz *et al*. 2007). In contrast, our data show that granule cells in Crus II have broad, widely convergent receptive fields (cf. Figs S4 and 6*A*), comparable to Golgi cells and Purkinje cells (see Holtzman *et al*. 2006 and Supplementary S5). Similar convergence has been reported by others (Thach, 1967; Eccles *et al*. 1971), prompting a re-evaluation of the fractured mosaic model.

The contrast of short- and long-lasting excitations in granule cells might be consistent with such activity patterns sub-serving different functions. Short-lasting excitations, at latencies similar to Golgi cells (see Supplementary Fig. S4), are well suited for the representation of spatial or temporally specific punctuate sensory events, whereas the persistent nature of the prolonged excitations may allow information processing on much longer timescales, and influence the responses to punctate sensory events from elsewhere. The influence of early and late depressions places particular timing constraints on granule cell activity. Our experiments did not directly address the mechanisms behind the

prolonged granule cell excitations, although their close correlation with Golgi cell depressions suggests that *dis-inhibition* plays an important role. Indeed, the granule cells generating the mGluR2-based depression of Golgi cell firing could generate *dis-inhibition* in other granule cells that target Purkinje cells and molecular layer interneurones. Purkinje cell output is closely correlated to prolonged granule cell activity, although Purkinje cell responses tend to last longer still. Since increased granule cell activity is correlated with spillover activation of mGluR2 in Golgi cells, similar activation of mGluR1/5 in Purkinje cells (Tempia *et al*. 1998) is a good potential candidate to explain this novel and unusual relationship.

Functional relevance of spillover-mediated control

The receptive fields and response dynamics of granule cells are closely correlated with Golgi cell behaviour. The delayed onset of granule cell prolonged excitation (∼110–150 ms, ∼50–100 ms after Golgi cell depressions begin) is roughly equivalent to a typical Golgi cell interspike interval and might reflect a requirement for a decline of spillover levels of GABA within the glomerulus. Golgi cell terminals sense these levels using $GABA_B$ auto-receptors, which reduce release probability (Mapelli *et al*. 2009). We hypothesise that long-lasting depressions in Golgi cells lead to increased release probability upon the resumption of their firing – this mechanism could explain the closely linked co-termination of prolonged granule cell/Golgi cell responses. Some granule cells showed late depressions (following prolonged excitations) which subsided within ∼500 ms (∼5 Golgi cell spikes). This may reflect a re-establishment of glomerular GABA equilibriums and/or changes in Golgi cell release probability perhaps supplemented by a relative gain-decrease in the granule cell input–output relationship as GABA levels rise (Mitchell & Silver, 2003).

Traditionally, Golgi cells have been considered to be negative-feedback controllers of granule cell activity (Eccles *et al*. 1966; Marr, 1969; Albus, 1971). Our findings suggest a very different mechanism. Specifically, we hypothesise that stimulus-evoked granule cell activity takes 'control' of Golgi cells through mGluR2-mediated inhibition. This coupling may counterbalance the phasic and tonic inhibition mediated by Golgi cells on mossy fibre transmission through granule cells. Thus, the Golgi–granule 'loop' can be thought as self-regulating via GABA spillover levels in the glomerulus, which have downstream effects on glutamate spillover in the molecular layer.

In many functions ascribed to the cerebellum e.g. delay conditioning, motor coordination or stimulus anticipation, prolonged activity is needed. The lack of understanding of slow timing mechanisms has attracted much speculation recently (see Medina & Mauk, 2000; Yamazaki & Tanaka, 2009). Intriguingly, learning rates in the classically conditioned eye blink are optimal over delays spanning 200–500 ms, with no learning for delays of less than 100 ms and declining rates for delays greater than 500 ms (Ohyama *et al*. 2003). Our granule cell prolonged excitations are on the same scale as these critical delay values, not beginning until ∼100–150 ms and terminating at ∼500 ms. These responses may therefore be of considerable interest for models of cerebellar learning and highlight the importance of spillover mechanisms during sensory processing.

References

Albus JS (1971). A theory of cerebellar function. *Math Biosci* **10**, 25–61.

Barbour B (1993). Synaptic currents evoked in Purkinje cells by stimulating individual granule cells. *Neuron* **11**, 759–769.

Barmack NH & Yakhnitsa V (2008). Functions of interneurons in mouse cerebellum. *J Neurosci* **28**, 1140–1152.

Bengtsson F & Jorntell H (2009). Sensory transmission in cerebellar granule cells relies on similarly coded mossy fiber inputs. *Proc Natl Acad Sci U S A* **106**, 2389–2394.

Brickley SG, Cull-Candy SG & Farrant M (1996). Development of a tonic form of synaptic inhibition in rat cerebellar granule cells resulting from persistent activation of $GABA_A$ receptors. *J Physiol* **497**, 753–759.

Chadderton P, Margrie TW & Hausser M (2004). Integration of quanta in cerebellar granule cells during sensory processing. *Nature* **428**, 856–860.

Cirone J & Salt TE (2001). Group II and III metabotropic glutamate receptors contribute to different aspects of visual response processing in the rat superior colliculus. *J Physiol* **534**, 169–178.

Crowley JJ, Fioravante D & Regehr WG (2009). Dynamics of fast and slow inhibition from cerebellar golgi cells allow flexible control of synaptic integration. *Neuron* **63**, 843–853.

D'Angelo E & De Zeeuw CI (2009). Timing and plasticity in the cerebellum: focus on the granular layer. *Trends Neurosci* **32**, 30–40.

Davey NJ, Ellaway PH & Stein RB (1986). Statistical limits for detecting change in the cumulative sum derivative of the peristimulus time histogram. *J Neurosci Methods* **17**, 153–166.

Dino MR, Willard FH & Mugnaini E (1999). Distribution of unipolar brush cells and other calretinin immunoreactive components in the mammalian cerebellar cortex. *J Neurocytol* **28**, 99–123.

Dugue GP, Brunel N, Hakim V, Schwartz E, Chat M, Levesque M, Courtemanche R, Lena C & Dieudonne S (2009). Electrical coupling mediates tunable low-frequency oscillations and resonance in the cerebellar Golgi cell network. *Neuron* **61**, 126–139.

Dugue GP, Dumoulin A, Triller A & Dieudonne S (2005). Target-dependent use of co-released inhibitory transmitters at central synapses. *J Neurosci* **25**, 6490–6498.

Dumoulin A, Triller A & Dieudonne S (2001). IPSC kinetics at identified GABAergic and mixed GABAergic and glycinergic synapses onto cerebellar Golgi cells. *J Neurosci* **21**, 6045–6057.

Eccles JC, Faber DS, Murphy JT, Sabah NH & Taborikova H (1971). Afferent volleys in limb nerves influencing impulse discharges in cerebellar cortex. I. In mossy fibers and granule cells. *Exp Brain Res* **13**, 15–35.

Eccles JC, Llinas R & Sasaki K (1966). The mossy fibre-granule cell relay of the cerebellum and its inhibitory control by Golgi cells. *Exp Brain Res* **1**, 82–101.

Eckhorn R & Thomas U (1993). A new method for the insertion of multiple microprobes into neural and muscular tissue, including fiber electrodes, fine wires, needles and microsensors. *J Neurosci Methods* **49**, 175–179.

Edgley SA & Lidierth M (1987). The discharges of cerebellar Golgi cells during locomotion in the cat. *J Physiol* **392**, 315–332.

Frey O, Holtzman T, McNamara RM, Theobald DE, van der Wal PD, de Rooij NF, Dalley JW & Koudelka-Hep M (2010). Enzyme-based choline and L-glutamate biosensor electrodes on silicon microprobe arrays. *Biosens Bioelectron* **26**, 477–484.

Gabbiani F, Midtgaard J & Knopfel T (1994). Synaptic integration in a model of cerebellar granule cells. *J Neurophysiol* **72**, 999–1009.

Gai Y & Carney LH (2008). Influence of inhibitory inputs on rate and timing of responses in the anteroventral cochlear nucleus. *J Neurophysiol* **99**, 1077–1095.

Holtzman T, Cerminara NL, Edgley SA & Apps R (2009). Characterization *in vivo* of bilaterally branching pontocerebellar mossy fibre to Golgi cell inputs in the rat cerebellum. *J Neurosci* **29**, 328–339.

Holtzman T, Rajapaksa T, Mostofi A & Edgley SA (2006). Different responses of rat cerebellar Purkinje cells and Golgi cells evoked by widespread convergent sensory inputs. *J Physiol* **574**, 491–507.

Iwamoto Y, Kaneko H, Yoshida K & Shimazu H (2009). Role of glycinergic inhibition in shaping activity of saccadic burst neurons. *J Neurophysiol* **101**, 3063–3074.

Jaarsma D, Dino MR, Ohishi H, Shigemoto R & Mugnaini E (1998). Metabotropic glutamate receptors are associated with non-synaptic appendages of unipolar brush cells in rat cerebellar cortex and cochlear nuclear complex. *J Neurocytol* **27**, 303–327.

Jakab RL & Hamori J (1988). Quantitative morphology and synaptology of cerebellar glomeruli in the rat. *Anat Embryol (Berl)* **179**, 81–88.

Jorntell H & Ekerot CF (2006). Properties of somatosensory synaptic integration in cerebellar granule cells *in vivo*. *J Neurosci* **26**, 11786–11797.

Kingston AE, Ornstein PL, Wright RA, Johnson BG, Mayne NG, Burnett JP, Belagaje R, Wu S & Schoepp DD (1998). LY341495 is a nanomolar potent and selective antagonist of group II metabotropic glutamate receptors. *Neuropharmacology* **37**, 1–12.

Kutscher A & Covey E (2009). Functional role of GABAergic and glycinergic inhibition in the intermediate nucleus of the lateral lemniscus of the big brown bat. *J Neurophysiol* **101**, 3135–3146.

Lujan R, Roberts JD, Shigemoto R, Ohishi H & Somogyi P (1997). Differential plasma membrane distribution of metabotropic glutamate receptors mGluR1α, mGluR2 and mGluR5, relative to neurotransmitter release sites. *J Chem Neuroanat* **13**, 219–241.

Ma D, Hongqi T, Hongbin S, Kozikowski AP, Pshenichkin S & Wroblewski JT (1997). Synthesis and biological activity of cyclic analogues of MPPG and MCPG as metabotropic glutamate receptor antagonists. *Bioorg Med Chem Lett* **7**, 1195–1198.

Maex R & De Schutter E (1998). Synchronization of golgi and granule cell firing in a detailed network model of the cerebellar granule cell layer. *J Neurophysiol* **80**, 2521–2537.

Mapelli L, Rossi P, Nieus T & D'Angelo E (2009). Tonic activation of $GABA_B$ receptors reduces release probability at inhibitory connections in the cerebellar glomerulus. *J Neurophysiol* **101**, 3089–3099.

Marr D (1969). A theory of cerebellar cortex. *J Physiol* **202**, 437–470.

Medina JF & Mauk MD (2000). Computer simulation of cerebellar information processing. *Nat Neurosci* **3**, 1205–1211.

Mitchell SJ & Silver RA (2000*a*). Glutamate spillover suppresses inhibition by activating presynaptic mGluRs. *Nature* **404**, 498–502.

Mitchell SJ & Silver RA (2000*b*). GABA spillover from single inhibitory axons suppresses low-frequency excitatory transmission at the cerebellar glomerulus. *J Neurosci* **20**, 8651–8658.

Mitchell SJ & Silver RA (2003). Shunting inhibition modulates neuronal gain during synaptic excitation. *Neuron* **38**, 433–445.

Mortensen M, Ebert B, Wafford K & Smart TG (2010). Distinct activities of GABA agonists at synaptic- and extrasynaptic-type $GABA_A$ receptors. *J Physiol* **588**, 1251–1268.

Mortensen M, Kristiansen U, Ebert B, Frolund B, Krogsgaard-Larsen P & Smart TG (2004). Activation of single heteromeric $GABA_A$ receptor ion channels by full and partial agonists. *J Physiol* **557**, 389–413.

Ohishi H, Ogawa-Meguro R, Shigemoto R, Kaneko T, Nakanishi S & Mizuno N (1994). Immunohistochemical localization of metabotropic glutamate receptors, mGluR2 and mGluR3, in rat cerebellar cortex. *Neuron* **13**, 55–66.

Ohyama T, Nores WL, Murphy M & Mauk MD (2003). What the cerebellum computes. *Trends Neurosci* **26**, 222–227.

Perroy J, Prezeau L, De Waard M, Shigemoto R, Bockaert J & Fagni L (2000). Selective blockade of P/Q-type calcium channels by the metabotropic glutamate receptor type 7 involves a phospholipase C pathway in neurons. *J Neurosci* **20**, 7896–7904.

Prsa M, Dash S, Catz N, Dicke PW & Thier P (2009). Characteristics of responses of Golgi cells and mossy fibers to eye saccades and saccadic adaptation recorded from the posterior vermis of the cerebellum. *J Neurosci* **29**, 250–262.

Rancz EA, Ishikawa T, Duguid I, Chadderton P, Mahon S & Hausser M (2007). High-fidelity transmission of sensory information by single cerebellar mossy fibre boutons. *Nature* **450**, 1245–1248.

Rossi DJ & Hamann M (1998). Spillover-mediated transmission at inhibitory synapses promoted by high affinity α6 subunit $GABA_A$ receptors and glomerular geometry. *Neuron* **20**, 783–795.

Sanchez JT, Gans D & Wenstrup JJ (2008). Glycinergic 'inhibition' mediates selective excitatory responses to combinations of sounds. *J Neurosci* **28**, 80–90.

Shambes GM, Gibson JM & Welker W (1978). Fractured somatotopy in granule cell tactile areas of rat cerebellar hemispheres revealed by micromapping. *Brain Behav Evol* **15**, 94–140.

Storustovu SI & Ebert B (2006). Pharmacological characterization of agonists at delta-containing $GABA_A$ receptors: Functional selectivity for extrasynaptic receptors is dependent on the absence of γ2. *J Pharmacol Exp Ther* **316**, 1351–1359.

Tempia F, Miniaci MC, Anchisi D & Strata P (1998). Postsynaptic current mediated by metabotropic glutamate receptors in cerebellar Purkinje cells. *J Neurophysiol* **80**, 520–528.

Thach WT Jr (1967). Somatosensory receptive fields of single units in cat cerebellar cortex. *J Neurophysiol* **30**, 675–696.

Thompson RF & Steinmetz JE (2009). The role of the cerebellum in classical conditioning of discrete behavioral responses. *Neuroscience* **162**, 732–755.

Van Welie I & Hausser M (2009). Sensory-driven excitation in cerebellar Lugaro cells revealed by in vivo targeted patch-clamp recordings. *2009 Abstract Viewer/Itinerary Planner*, Programme No. 367.18/DD40. Society for Neuroscience, Washington, DC.

Vervaeke K, Lorincz A, Gleeson P, Farinella M, Nusser Z & Silver RA (2010). Rapid desynchronization of an electrically coupled interneuron network with sparse excitatory synaptic input. *Neuron* **67**, 435–451.

Vos BP, Volny-Luraghi A & De Schutter E (1999). Cerebellar Golgi cells in the rat: receptive fields and timing of responses to facial stimulation. *Eur J Neurosci* **11**, 2621–2634.

Watanabe D & Nakanishi S (2003). mGluR2 postsynaptically senses granule cell inputs at Golgi cell synapses. *Neuron* **39**, 821–829.

Yamamoto C, Yamashita H & Chujo T (1976). Inhibitory action of glutamic acid on cerebellar interneurones. *Nature* **262**, 786–787.

Yamazaki T & Tanaka S (2009). Computational models of timing mechanisms in the cerebellar granular layer. *Cerebellum* **8**, 423–432.

Yeo CH & Hesslow G (1998). Cerebellum and conditioned reflexes. *Trends Cogn Sci* **2**, 322–330.

Author's present address

O. Frey: Bio Engineering Laboratory, Dept of Biosystems Science and Engineering, ETH Zurich, 4058 Basel, Switzerland.

Author contributions

All experiments were performed in the Dept of Physiology, Development and Neuroscience, Cambridge University. Conception and design of experiments: T.H. Collection, analysis and interpretation of data: T.H., V.S., T.Z., O.F. Drafting the article or revising it critically for important intellectual content: T.H., O.F., P.D.v.d.W., M.K.-H., J.W.D. and S.A.E. All authors approved the final version.

Acknowledgements

This study was in part supported by the European Commission under the Framework 6 Programme (Neuroprobes LSHM-CT-2006-27017). The funders had no role in study design, data collection and analysis, decision to publish, or preparation of the manuscript. The authors express their gratitude to Dr Abteen Mostofi, Cambridge University, for experimental and histological assistance.